Hard X-ray Photoelectron Spectroscopy of $Hg_2Ru_2O_7$ and $Tl_2Ru_2O_7$

A. Chainani[A], A. Yamamoto[B], M. Matsunami[A], R. Eguchi[A], M. Taguchi[A], Y. Takata[A], Y. Ishida[A], T. Baba[A], Y. Senba[C], H. Ohashi[C], M. Yabashi[A], Y. Nishino[A], K. Tamasaku[A], T. Ishikawa[A,C], H. Takagi[B,D] and S. Shin[A,E]

RIKEN/SPring-8[A], RIKEN/Wako[B], JASRI/SPring-8[C], Univ. Tokyo[D], ISSP[E]

$Hg_2Ru_2O_7$ and $Tl_2Ru_2O_7$ exhibit first order metal-insulator transitions

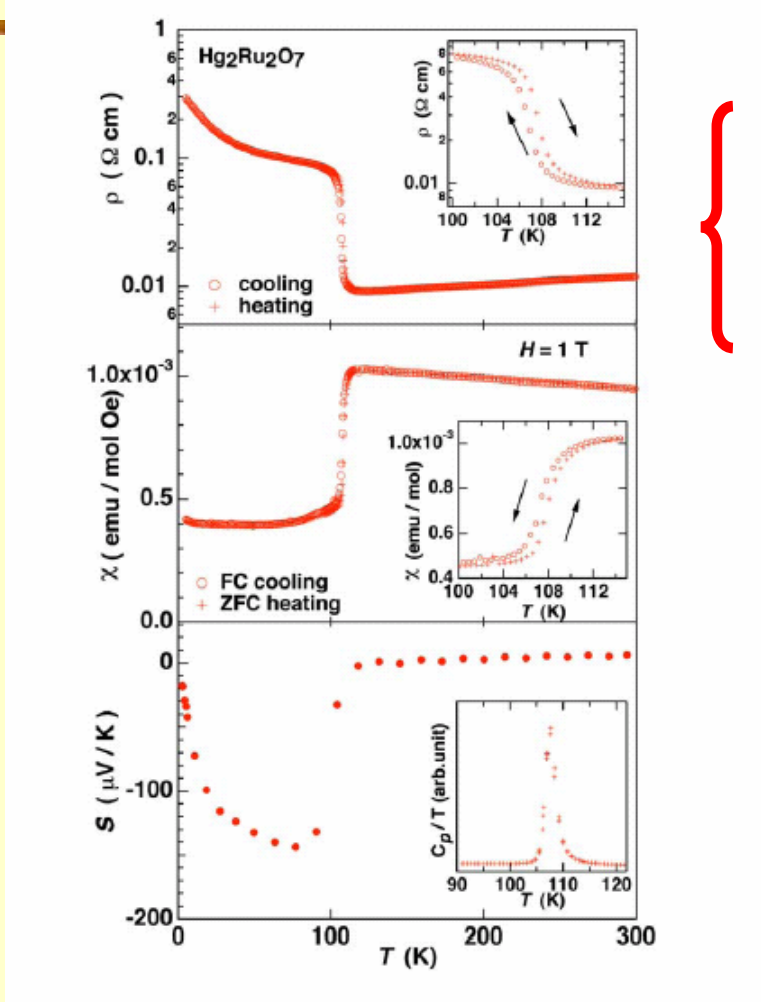

- $Hg_2Ru_2O_7$
- Tc = 108 K
- μ_{eff} ~3.7μ_B

- $Tl_2Ru_2O_7$
- Tc = 125 K
- μ_{eff} ~ 2.8μ_B

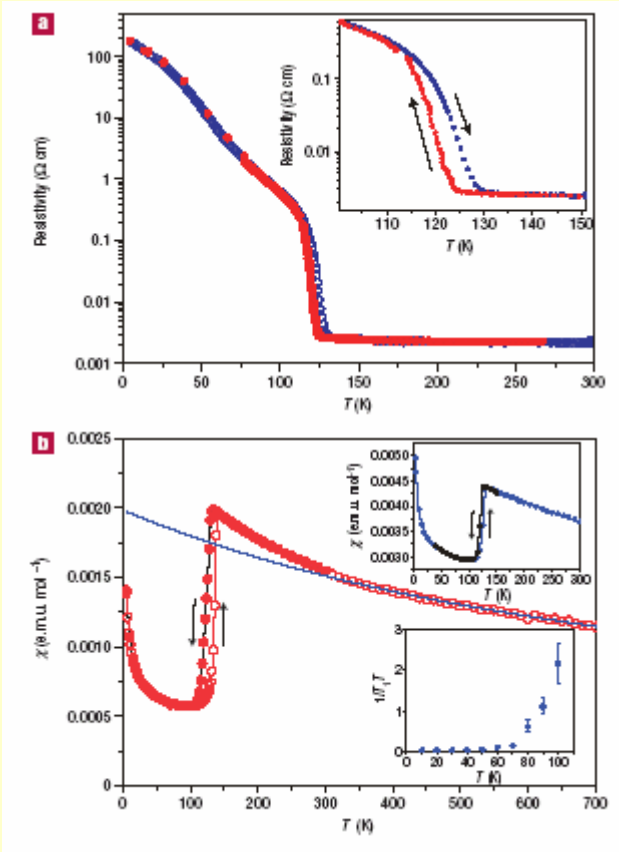

A Yamamoto et al JPSJ(Letters) 4, 043703 (2007)
W. Klein et al J. Mat. Chemistry 17, 1356 (2007)

S. Lee et al Nature Materials 5, 471 (2006)

Spin gap in $Tl_2Ru_2O_7$ and the possible formation of Haldane chains in three-dimensional crystals

SEONGSU LEE[1], J.-G. PARK[1,2]*, D. T. ADROJA[3], D. KHOMSKII[4], S. STRELTSOV[5], K. A. McEWEN[6], H. SAKAI[7], K. YOSHIMURA[7], V. I. ANISIMOV[5], D. MORI[8], R. KANNO[8] AND R. IBBERSON[3]

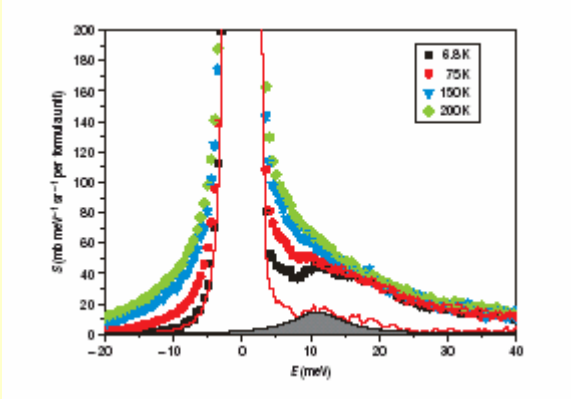

In low T phase, orthorhombic distortion

two types of Ru ions, no dimers but chains

with spin gap : S = 1 Haldane chains

LDA + U calculations indicate orbital order

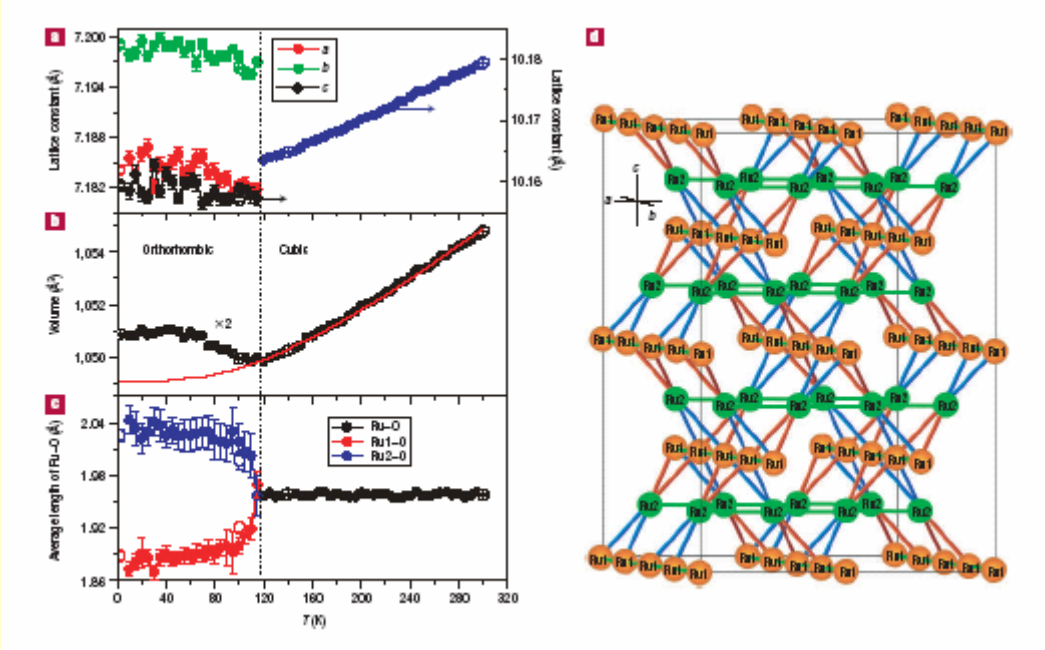

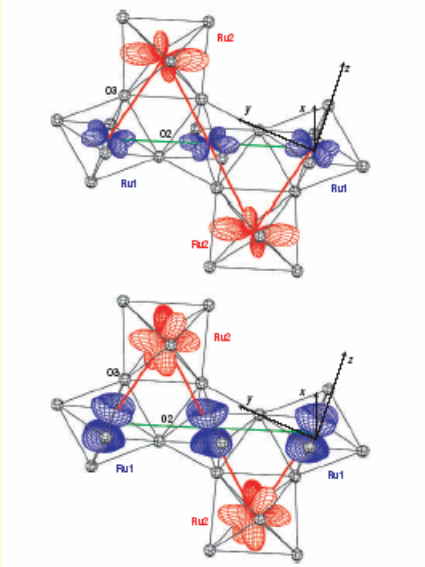

Figure 4 Orbital ordering in the low-temperature phase of $Tl_2Ru_2O_7$, obtained from LDA + U calculations. The electronic configuration of Ru^{4+} ions is $t_{2g}^2 \uparrow t_{2g}^1 \downarrow$. Hence, one of the t_{2g} orbitals will be fully occupied and inactive in the exchange interactions (top). The other two orbitals will be active (bottom). Orbitals of Ru2 (Ru1) are coloured red (blue). A local coordinate system whose axes point along Ru–O bonds is presented for one of the RuO_6 octahedra.

S. Lee et al Nature Materials 5, 471 (2006)

Is the MIT similar ?

- $Hg_2Ru_2O_7$: Ru 5+ 3 t_{2g} electrons => orbital order ✗
- $Tl_2Ru_2O_7$: Ru 4+ 4 t_{2g} electrons => orbital order ✓
- As yet, no direct experimental evidence for Orbital order(OO) driven MIT in $Tl_2Ru_2O_7$
- Is the MIT of the Mott-Hubbard type in both cases or not ?
- Ca_2RuO_4 and $La_4Ru_2O_{10}$ show OO in the insulating phase
- Note : $La_4Ru_2O_{10}$ has OO, but no MIT.

T. Mizokawa et al PRL 87, 077202(2001) ; H. Wu et al. PRL 96, 256402 (2006)
P Khalifah et al Science 297, 2237(2002)

Experiments

- High quality samples using high pressure synthesis, show sharp MIT
- Characterized by x-ray diffraction, electrical resistivity, magnetic susceptibility
- Photoemission / X-ray absorption experiments at beamline BL29XU / BL17SU @Spring 8.
- Energy resolution 230meV @ hν ~ 7.93 keV
- For XAS : 30 meV@500 eV
  energy stability better than 10 meV
- Temperature cycling for reproducibility

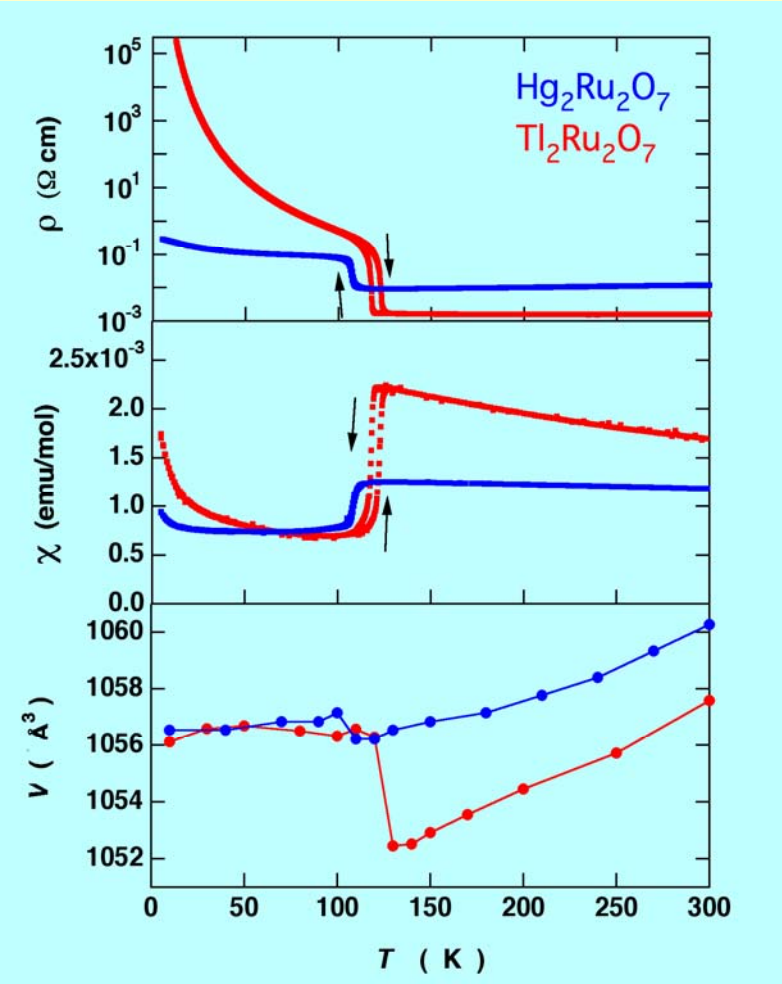

A Yamamoto

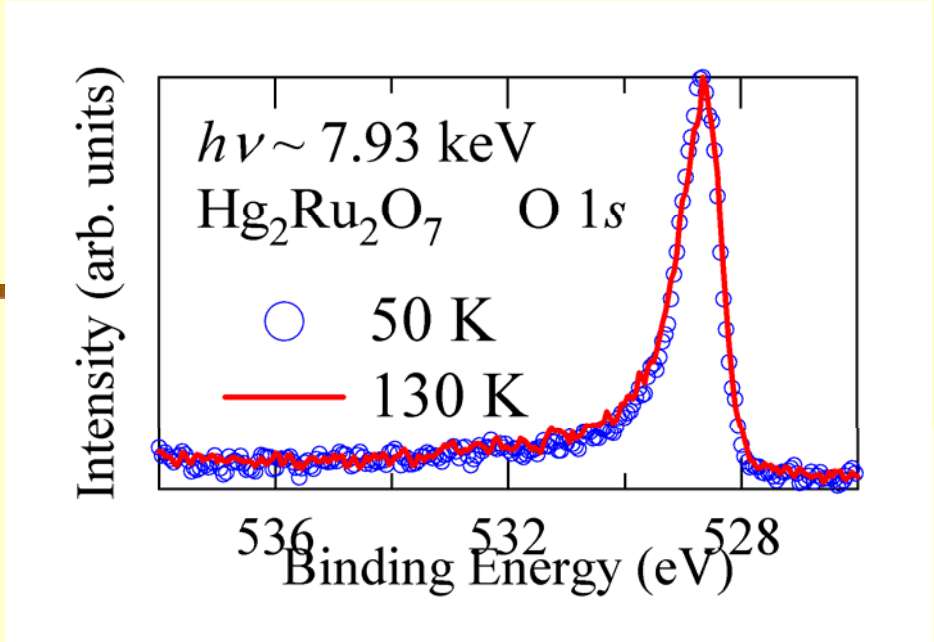

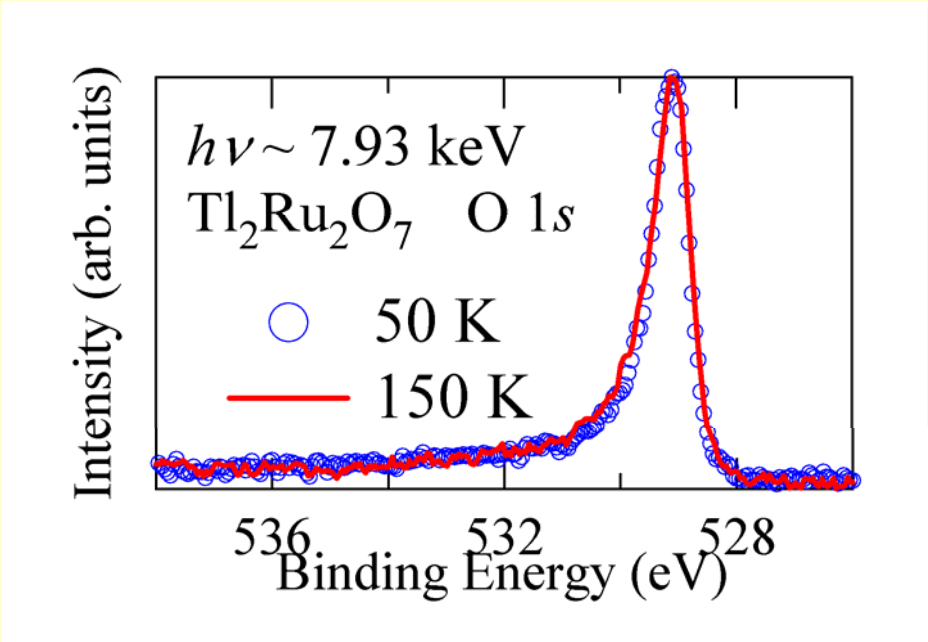

- O1s core level spectra in the metallic and insulating phases show no core level shifts
- No temperature dependence

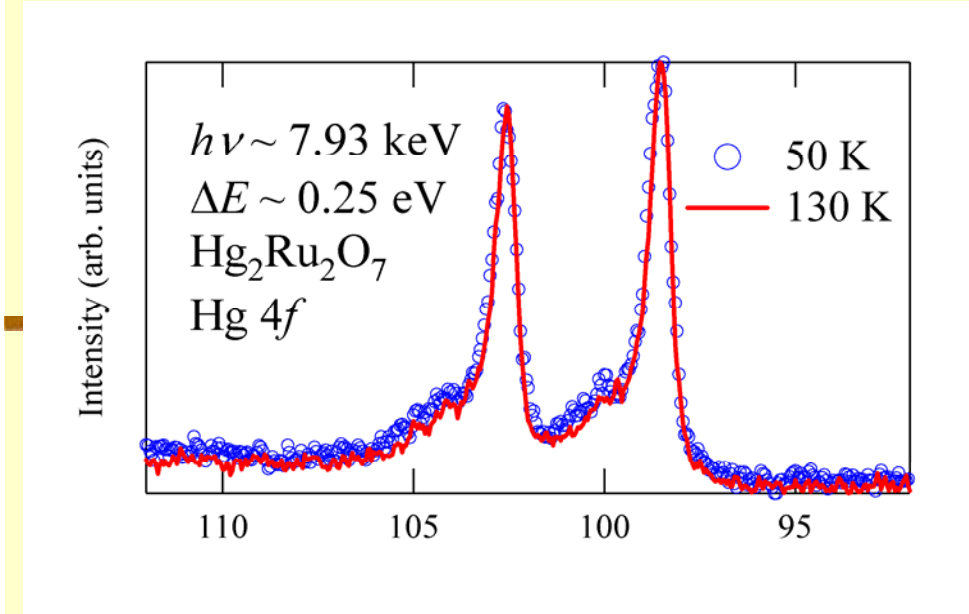

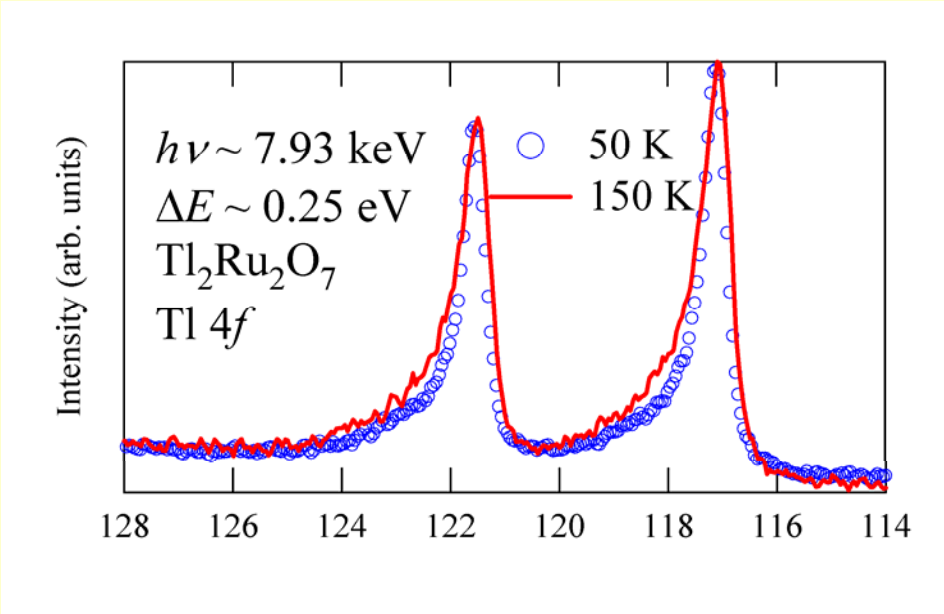

- Hg 4f and Tl 4f core level spectra in the metallic and insulating phases show no core level shifts
- Weak line shape change across MIT

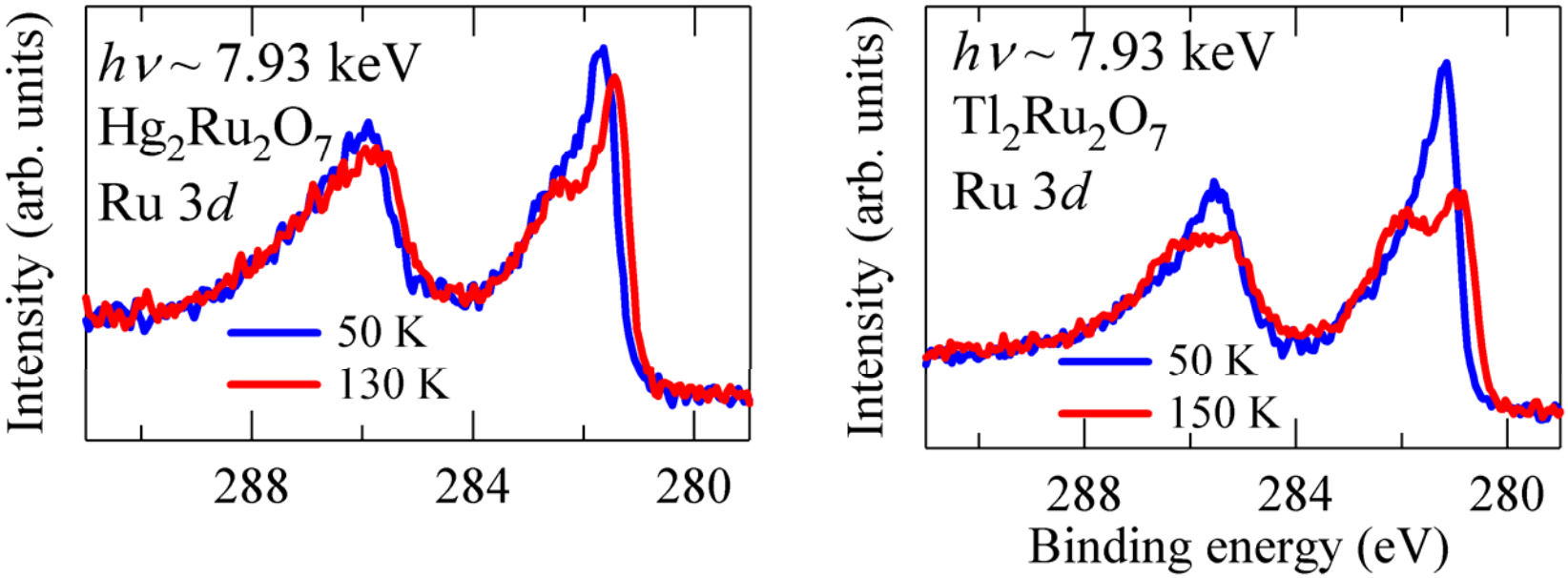

- Ru 3d core level spectra in the metallic and insulating phases show clear temperature dependence.

Core-level XPS satellites in ruthenates revealing the Mott-transition

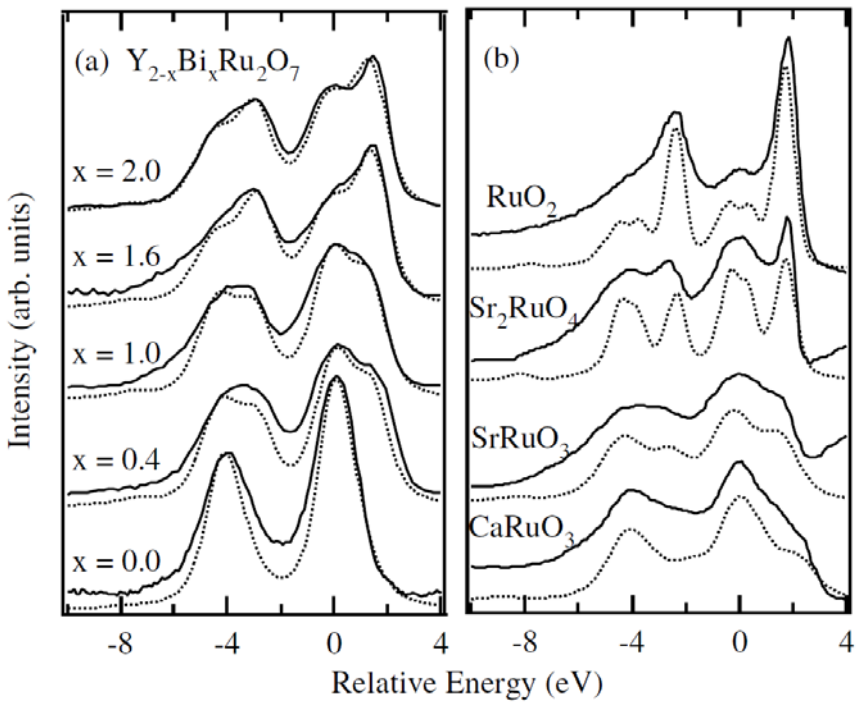

FIG. 5. Comparison of Ru 3*d* XPS spectra (solid lines) of (a) $Y_{2-x}Bi_xRu_2O_7$ and (b) other ruthenates with the present model calculations (dotted lines). See text for details.

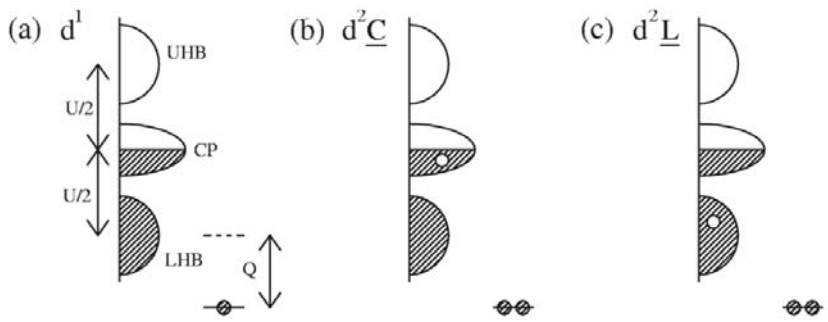

FIG. 4. Schematic diagrams of three major valence-electron configurations contributing to the core-level spectra. Note that the impurity level at the core-hole site is lowered by the attractive Coulomb potential Q.

H D Kim et al PRL **93**, 126404 (2004)

Valence and core levels of V_2O_3, G. Panaccione et al PRL 97, 116401 (2006)

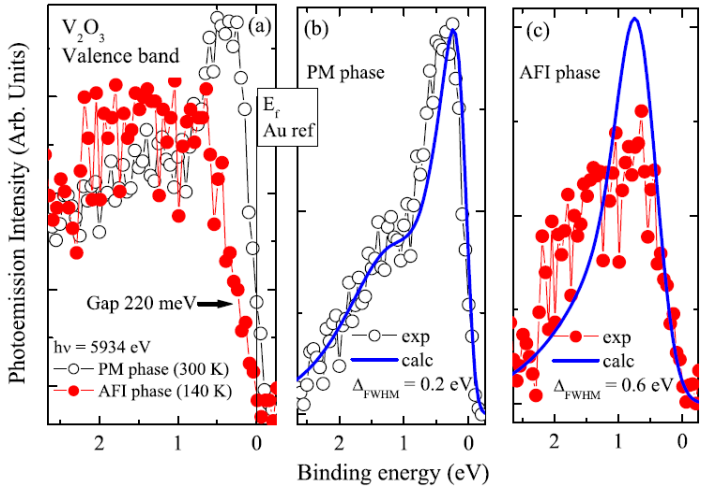

FIG. 1 (color online). Valence band spectra in the PM (white circles) and AFI (filled red circles) phase. (a) Raw data with no background subtraction. After subtraction of an integral background, spectra of panel (a) are compared with DMFT calculations for the PM phase (panel b) and for the AFI phase (panel c). To match the leading edge of the experimental data, calculated line shapes are convoluted with a Gaussian whose FWHM is $\Delta = 0.25$ eV (PM phase) or $\Delta = 0.6$ eV (AFI phase).

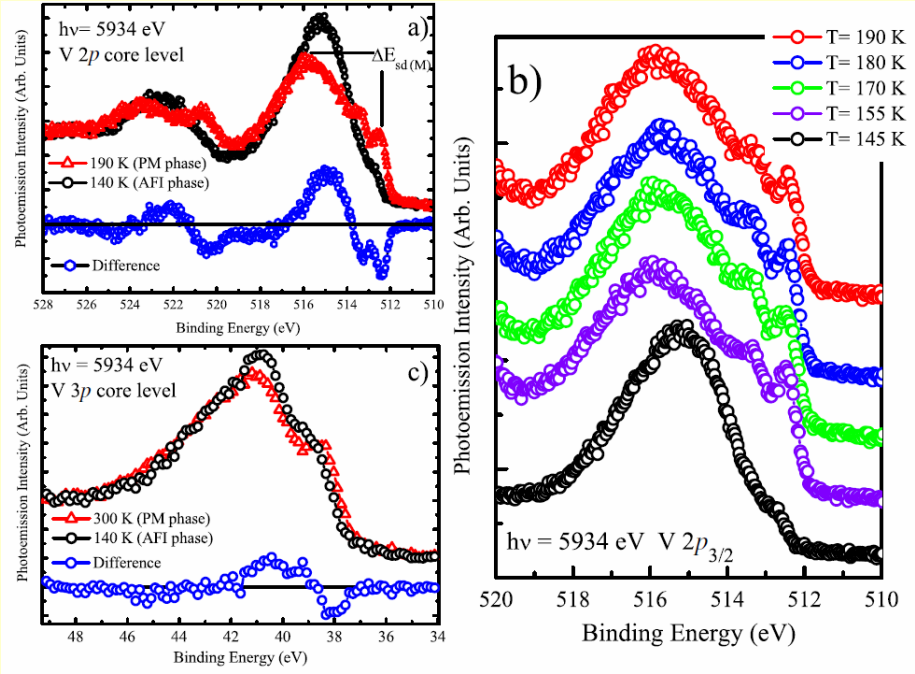

See also Soft x-ray PES of V_2O_3,
S. K Mo et al. PRL 97, 116401 (2006)

Valence band spectra

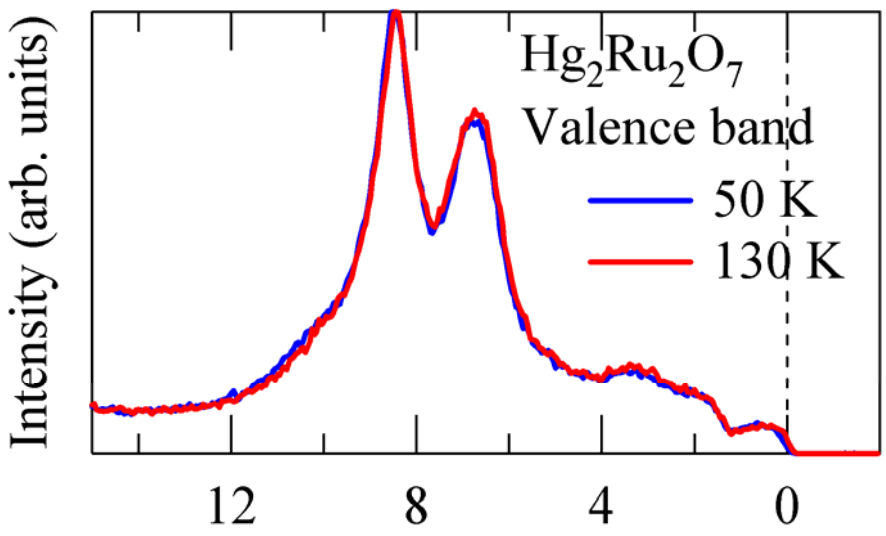

Small clear gap of ~70 meV

No shift in Hg 5d core levels

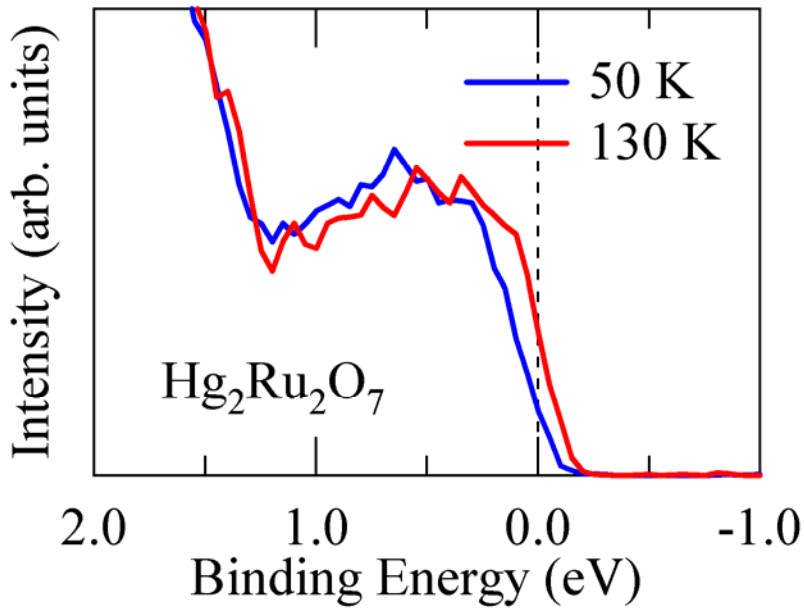

O 1s XAS spectra

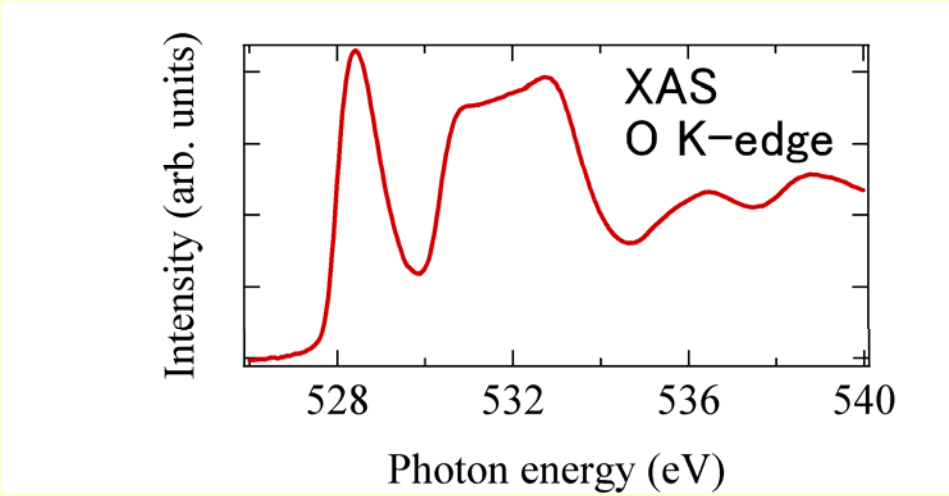

- Small gap also in unoccupied DOS of ~0.05 eV

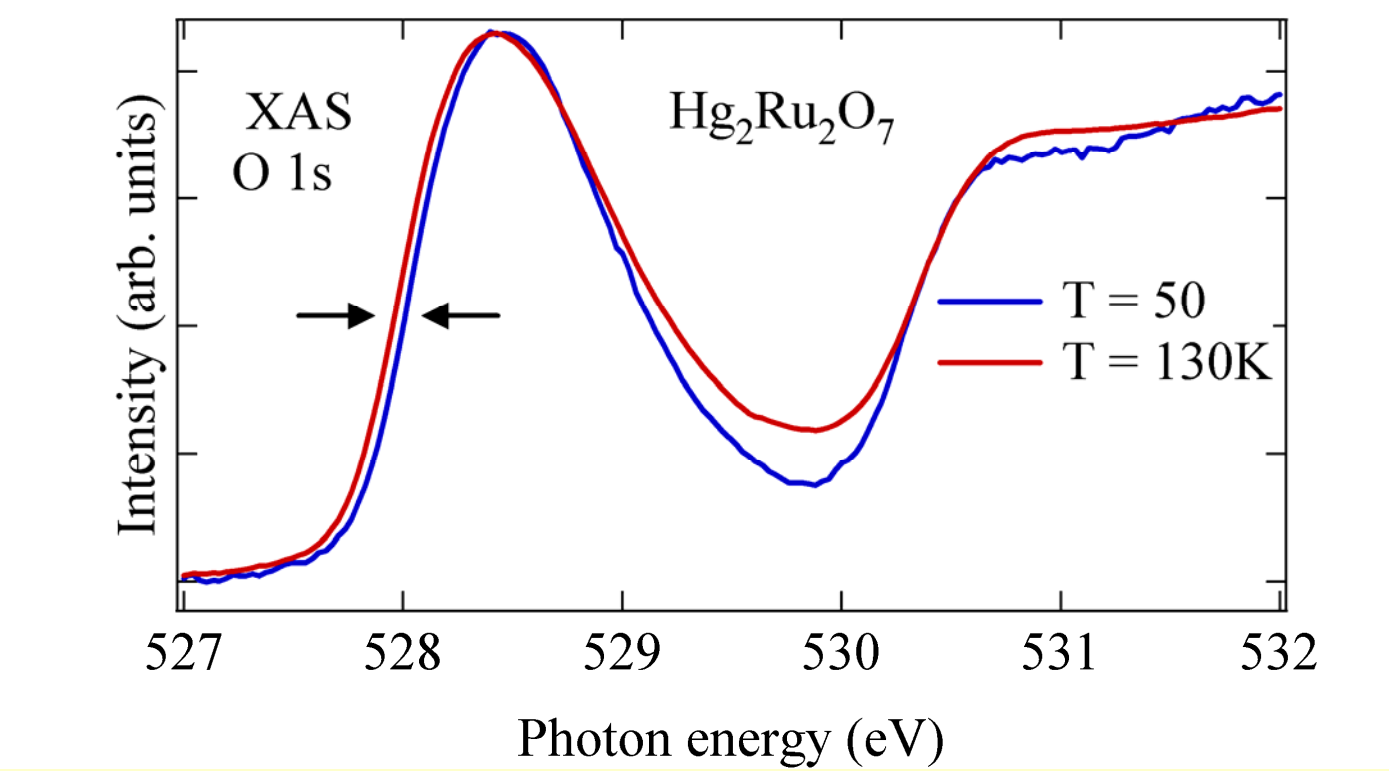

Valence band spectra

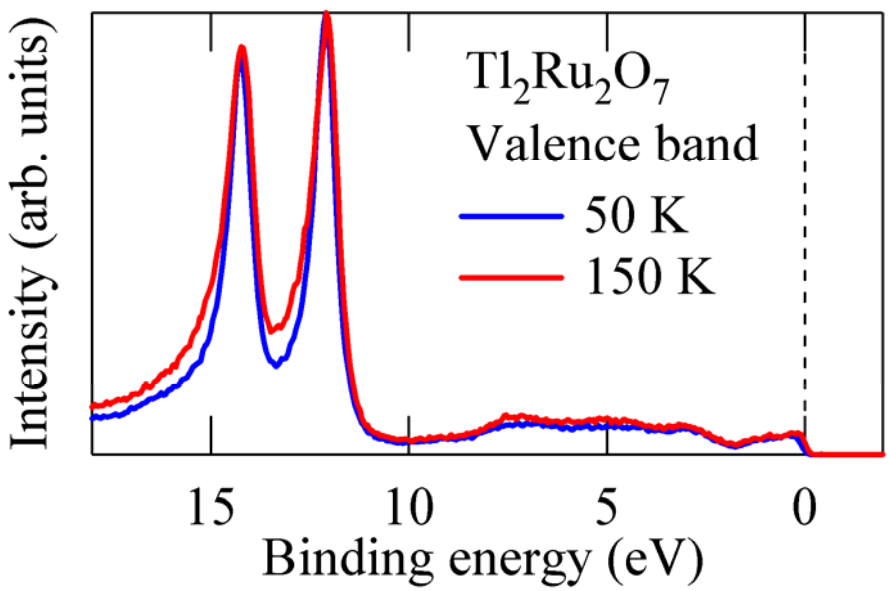

Clear gap formation ~0.1 eV

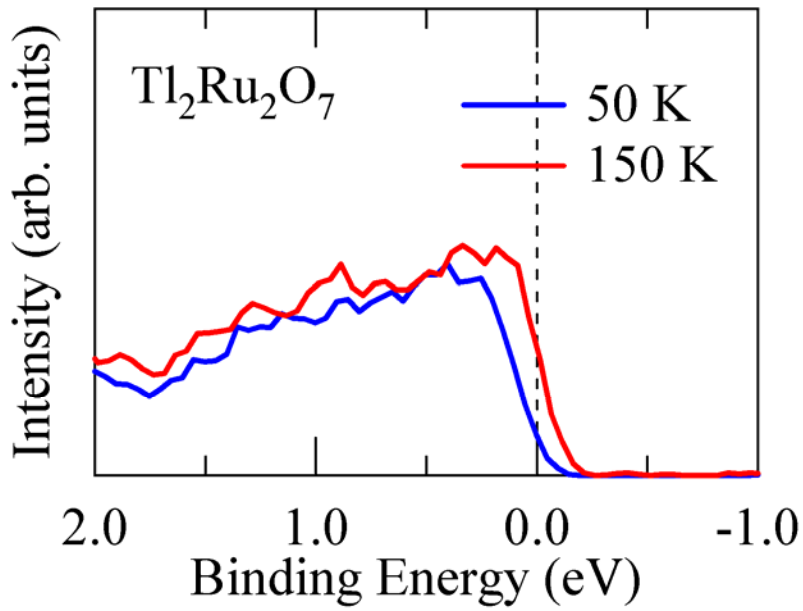

No shift in Tl 5d core levels

O 1s XAS spectra

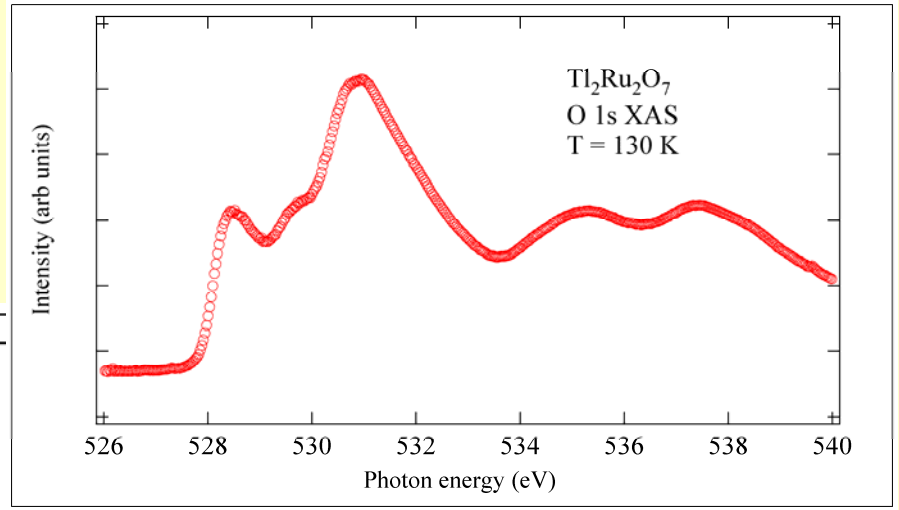

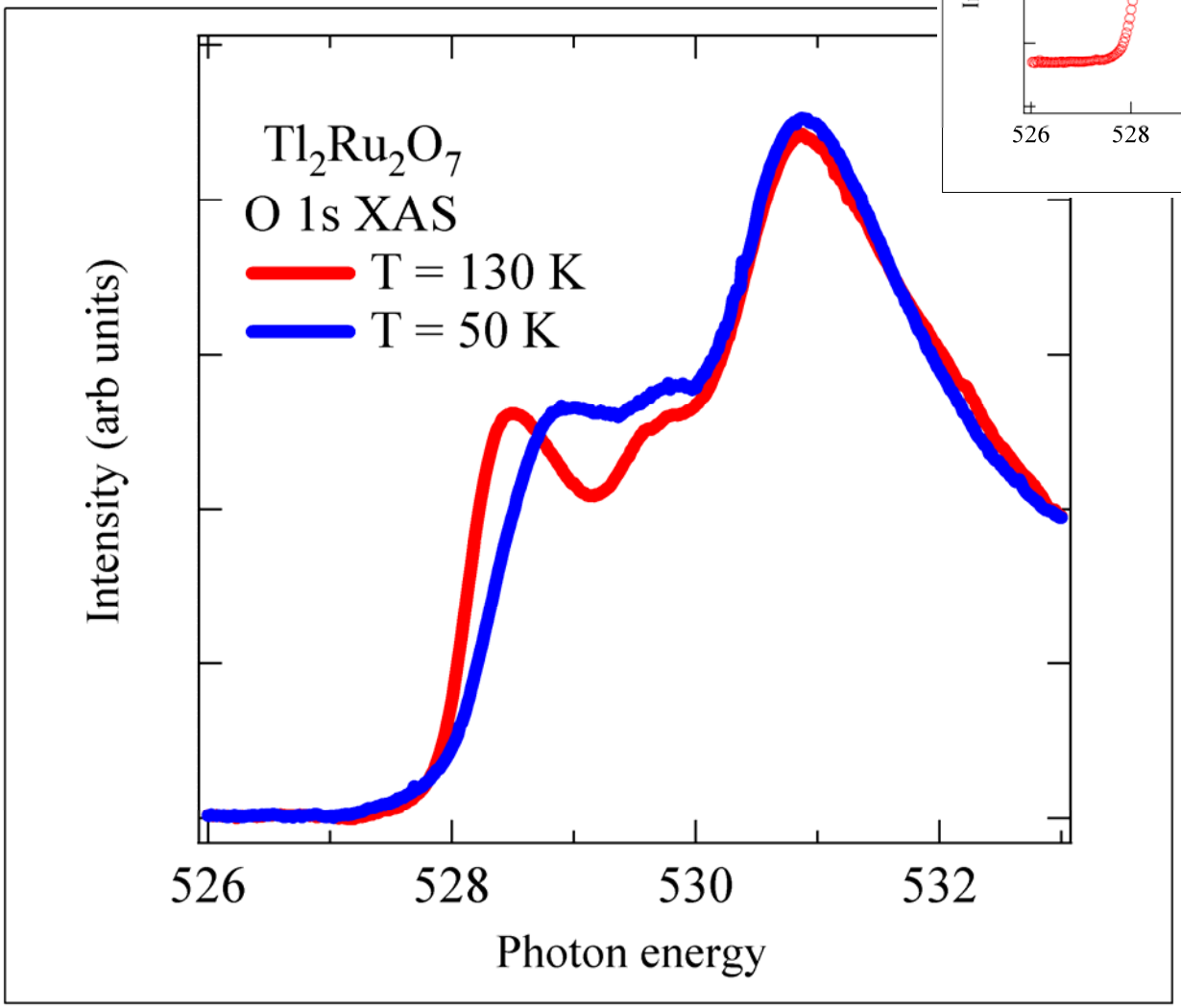

- Small gap also in unoccupied DOS ~0.1 eV

Occupied : Unoccupied

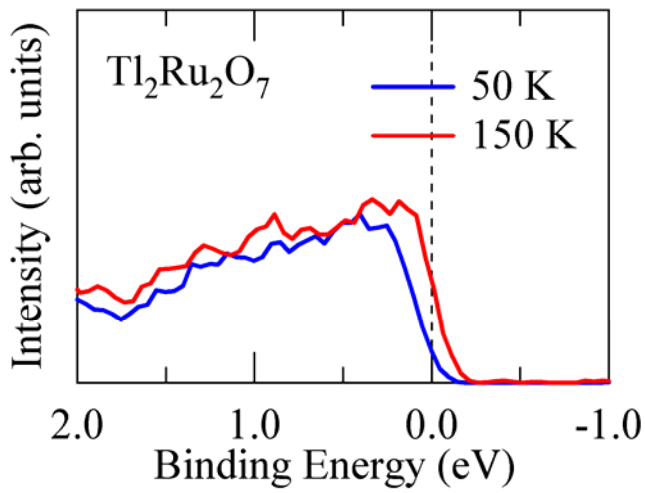

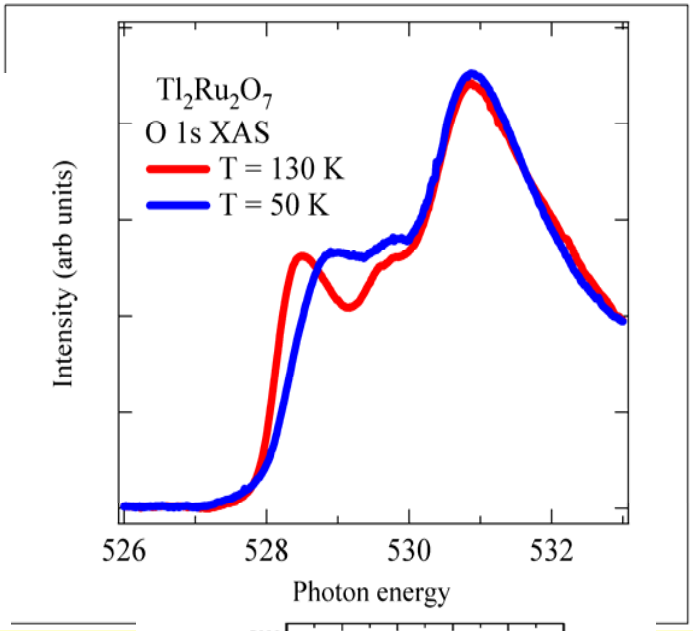

Total gap of ~0.2 eV,
much larger than spin gap
of 11 meV,
but consistent with
Optical spectroscopy

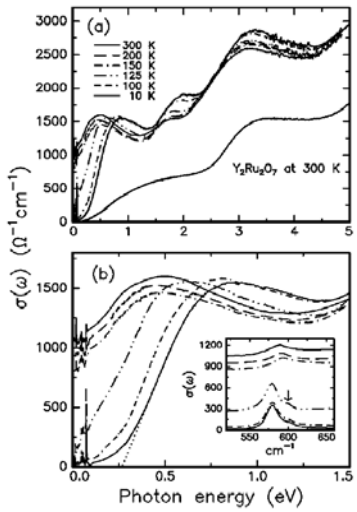

FIG. 2. (a) The $\sigma(\omega)$ of $Tl_2Ru_2O_7$ at various temperatures and the $\sigma(\omega)$ of $Y_2Ru_2O_7$ at room temperature, and (b) the detailed $\sigma(\omega)$ of $Tl_2Ru_2O_7$ in the low frequency region. The inset of (b) shows the T-dependent far-IR $\sigma(\omega)$ near the stretching phonon mode.

Optical
Spectroscopy

J Lee et al, PRB
64, 165108(2001)

Comparison with orbital ordering within the insulating phase of Ca_2RuO_4

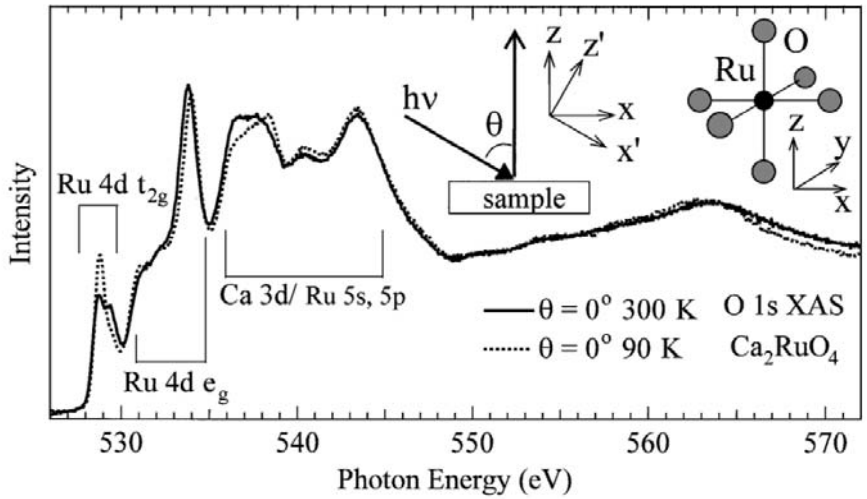

FIG. 1. O 1*s* x-ray absorption spectra of Ca_2RuO_4 taken at 90 and 300 K at normal incidence. The spectra are normalized using the higher energy region above 550 eV. The insets show schematic pictures of the experimental arrangement and the RuO_6 octahedron.

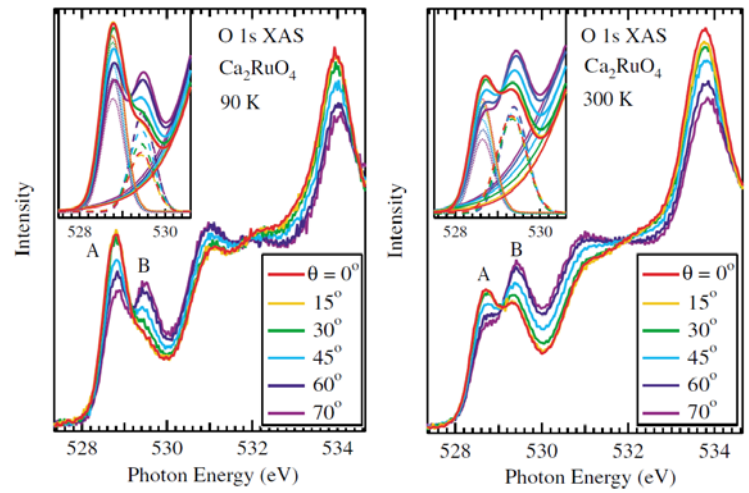

FIG. 2 (color). O 1*s* x-ray absorption spectra of Ca_2RuO_4 taken at 90 and at 300 K as a function of angle θ, which is the angle between the surface normal and the Poynting vector of the circularly polarized light. The spectra are normalized using the higher energy region above 550 eV. In the insets, the fitted results are shown by the thick solid curves. The two Gaussians for structures *A* and *B*, and the tail of another Gaussian for the e_g band are shown by the dotted, dashed, and solid curves, respectively.

Role of spin-orbit coupling in the Mott insulator
T. Mizokawa et al PRL 87, 077202(2001)

Resonant X-ray diffraction(L_3-edge) showed a T_{oo} = 260 K
I. Zegkinoglou et al PRL 95, 136401(2005)

Comparison with orbital ordering within the insulating phase of $La_4Ru_2O_{10}$

- Orbitally Driven Spin-Singlet Dimerization in S=1 $La_4Ru_2O_{10}$

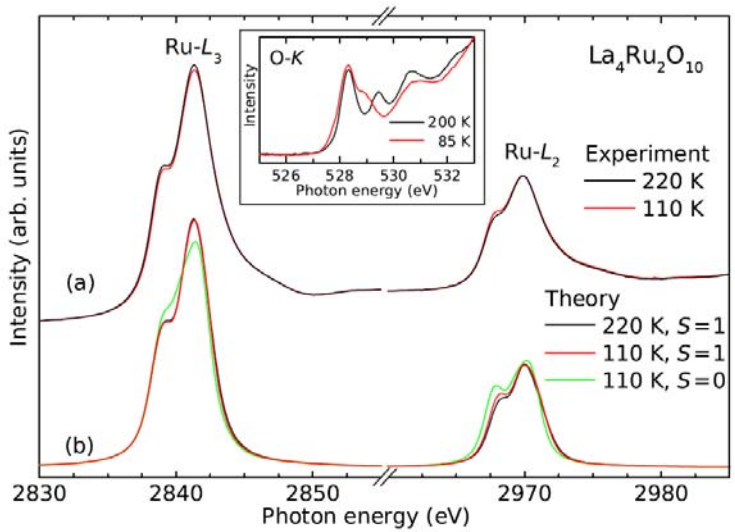

FIG. 2 (color online). (a) Experimental Ru-$L_{2,3}$ XAS spectra of $La_4Ru_2O_{10}$ measured at 220 and 110 K, i.e., above and below T_s = 160 K. (b) Theoretical simulations for the Ru^{4+} ion in the S = 1 high-temperature phase at 220 K, S = 1 low-temperature phase at 110 K, and S = 0. The inset shows O-K spectra measured at 200 and 85 K from [16].

H. Wu et al. PRL 96, 256402 (2006)

P Khalifah et al Science 297, 2237 (2002)

Local and non-local screening in ruthenates

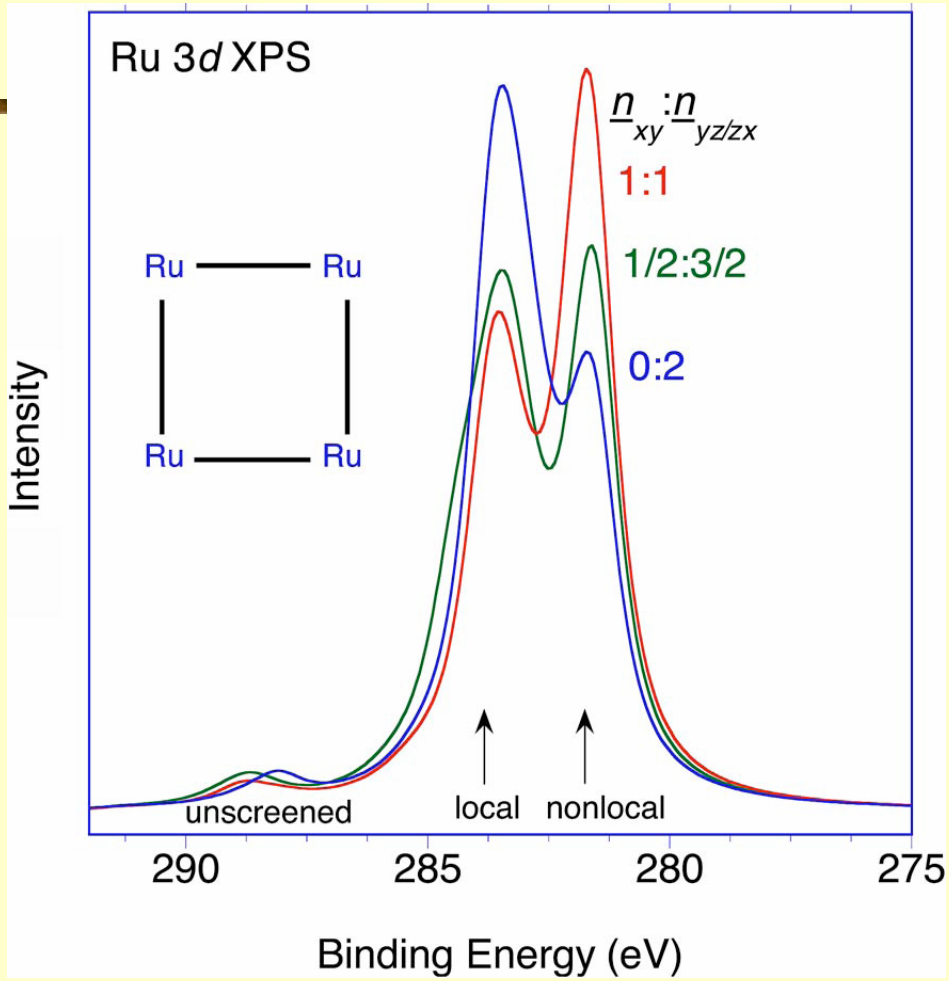

Orbital ordering in Ru 3d XPS of Ru_4 cluster

Low binding energy feature corresponds to the non-local screening

M. van Veenendaal
PRB 74, 085118 (2006)

M. van Veenendaal & G. A. Sawatzky
PRL 70, 2459 (1993)

Comparison with MIT in $Sm_{2-x}Bi_xRu_2O_7$

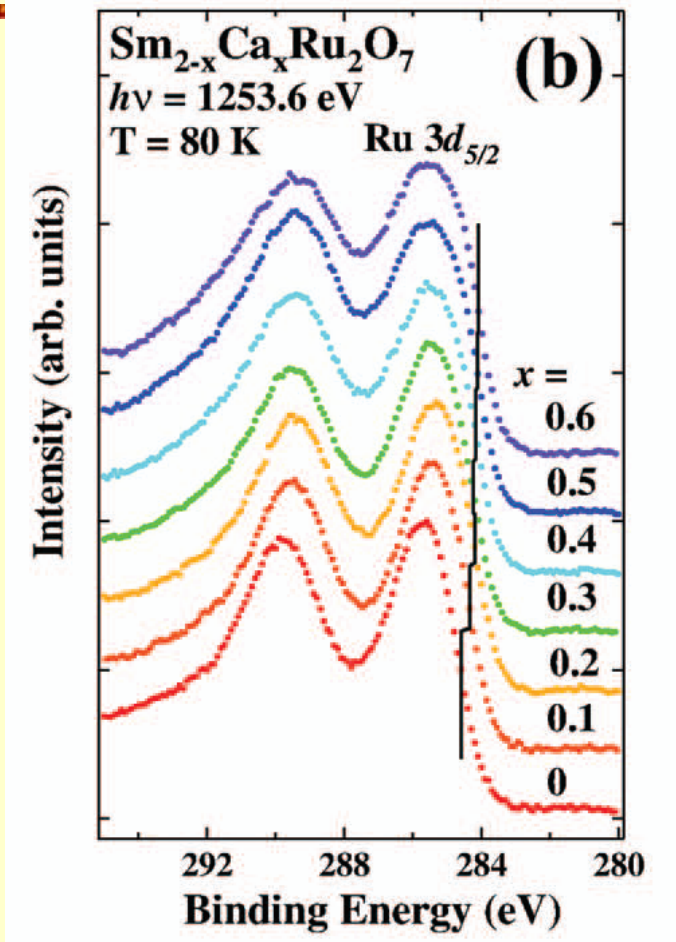

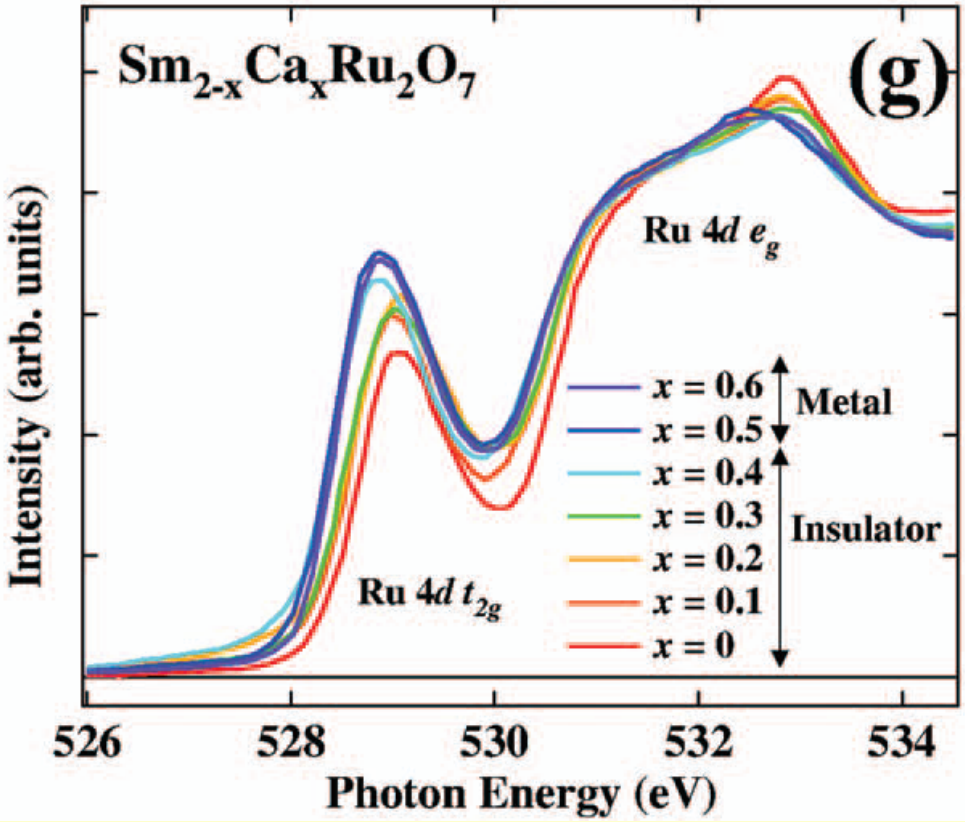

J Okamoto et al PRB 73, 035127(2006)

Comparison with earlier work on $Tl_2Ru_2O_7$

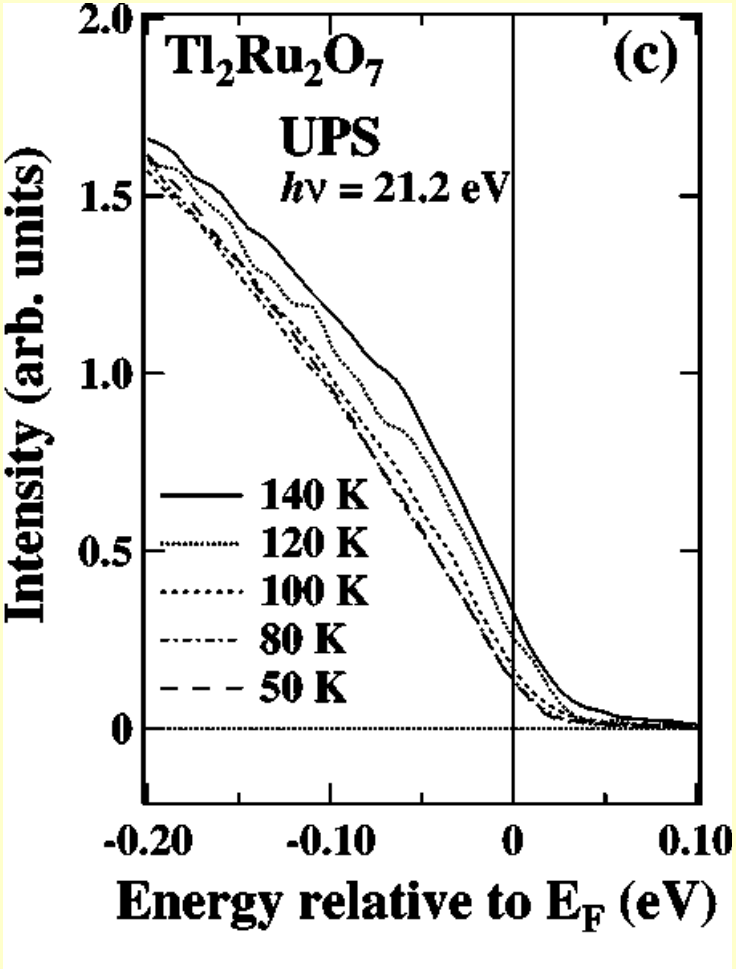

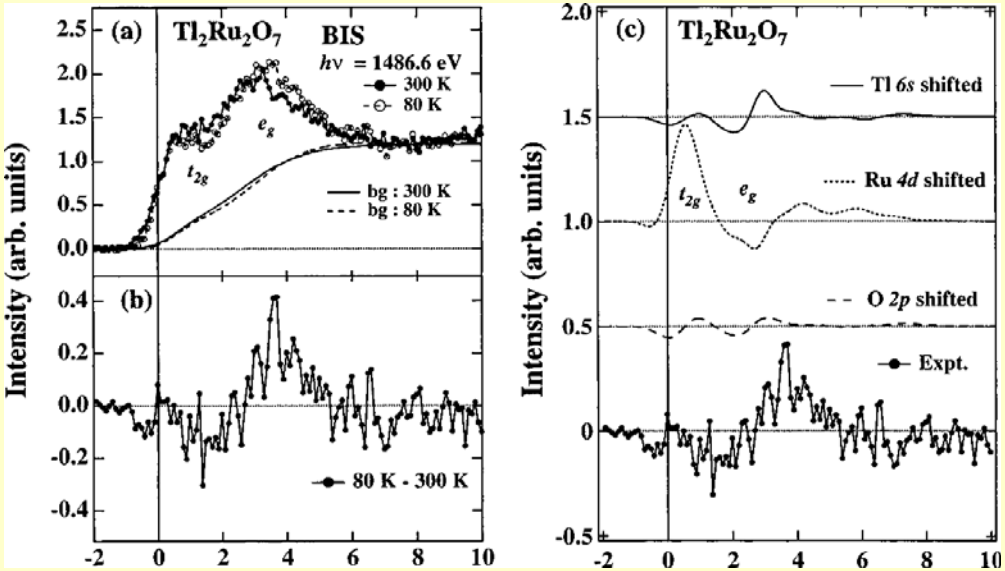

Ru 3d core levels not reported

J Okamoto et al PRB 69 035115(2004)

Cluster model calculations

Ground state : linear combination of 6 configurations

$3d^6\underline{C}^2$

$3d^5\underline{C} \longleftrightarrow 3d^6\underline{LC}$

$3d^4 \longleftrightarrow 3d^5\underline{L} \longleftrightarrow 3d^6\underline{L}^2$

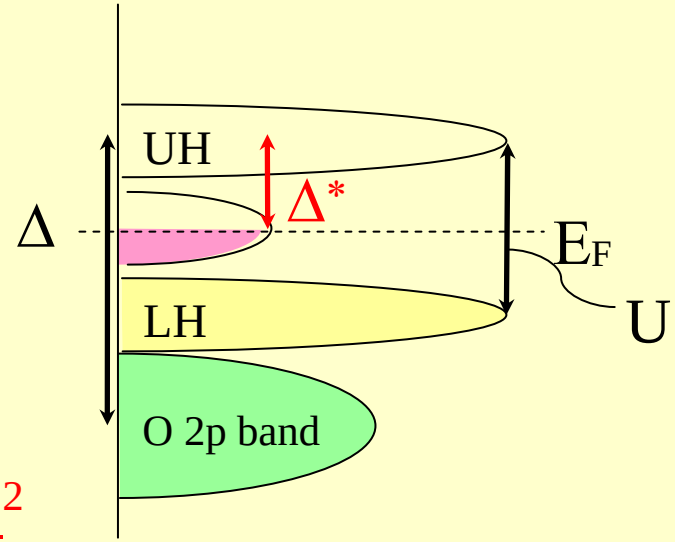

1. Intra-atomic multiplets

2. Crystal Field

3. Hybridization between O 2p and Ru 3d orbital

4. Hybridization between coherent states at E_F and Ru 3d orbitals

M. Taguchi

J. Imer & E. Wuilloud. Z Phys. B 66, 153 (1987)

Cluster model analysis

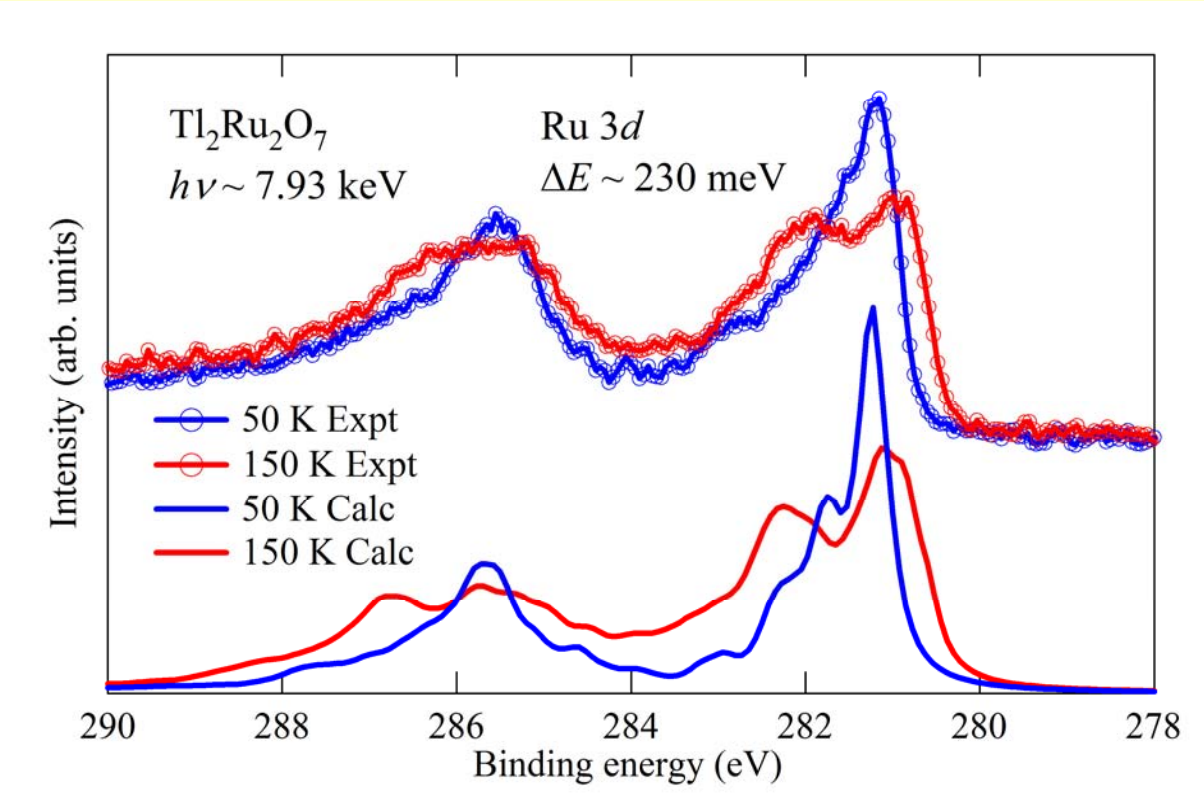

Parameters
$U = 3.0$ eV
$10Dq = 2.5$ eV
$\Delta = 7.0$ eV
$\Delta^* = 0.1$ eV
$V = 2.2$ eV
$V^* = 0.55$ eV

- Works fairly well
- Insulating phase : Only V* set to 0

Cluster model analysis for $Hg_2Ru_2O_7$.

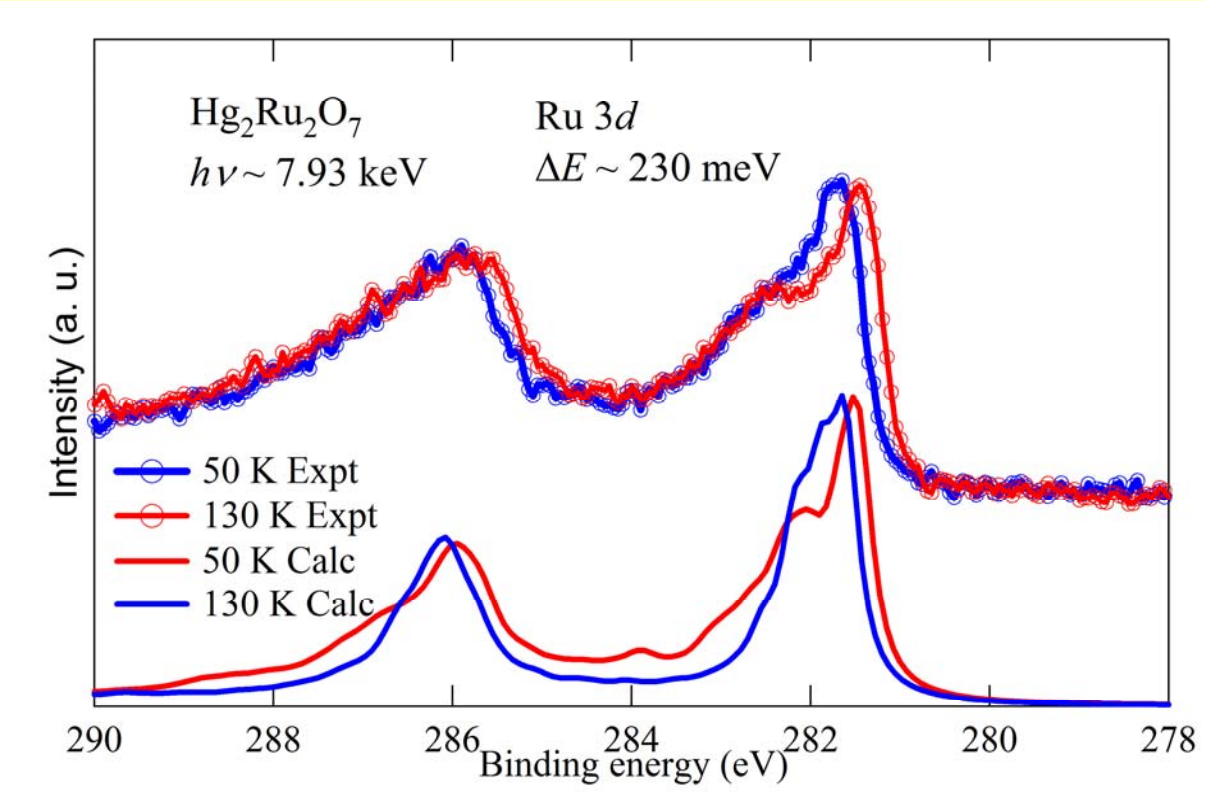

Parameters

	Hg	*Tl*
U = 3.0 eV		3.0 eV
$10Dq$ = 3.8 eV		2.5 eV
Δ =4.5 eV		7.0 eV
Δ^* = 0.1 eV		0.1 eV
V = 2.0 eV		2.2 eV
V^* = 0.94 eV		0.55 eV

LDA & LDA + DMFT of $Hg_2Ru_2O_7$

Importance of multi-orbital correlations

negligible influence of spin-orbit coupling

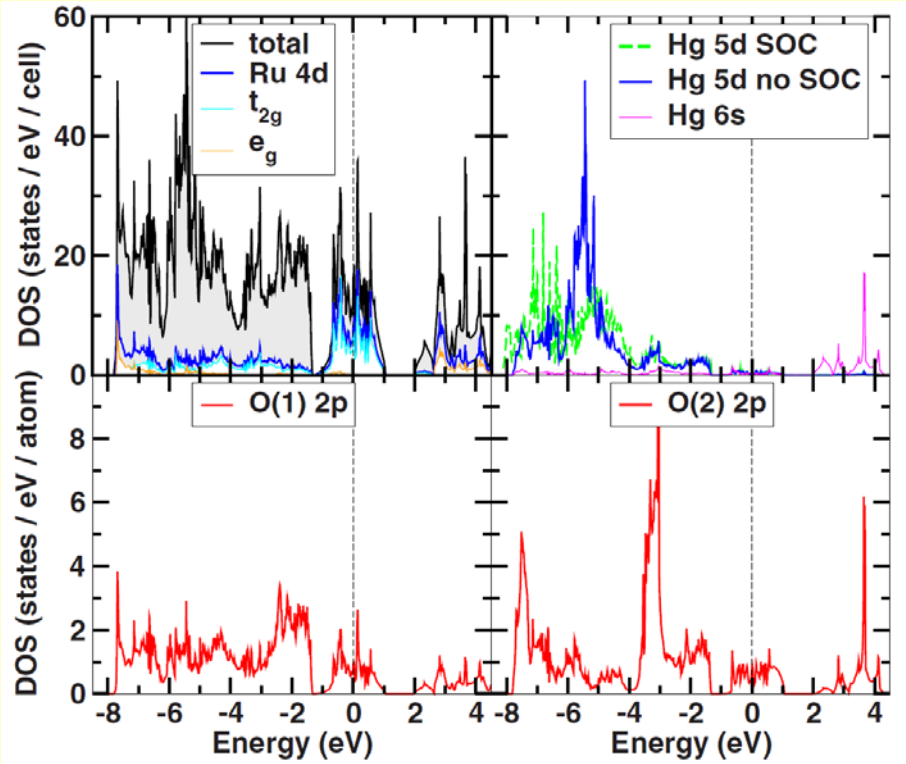

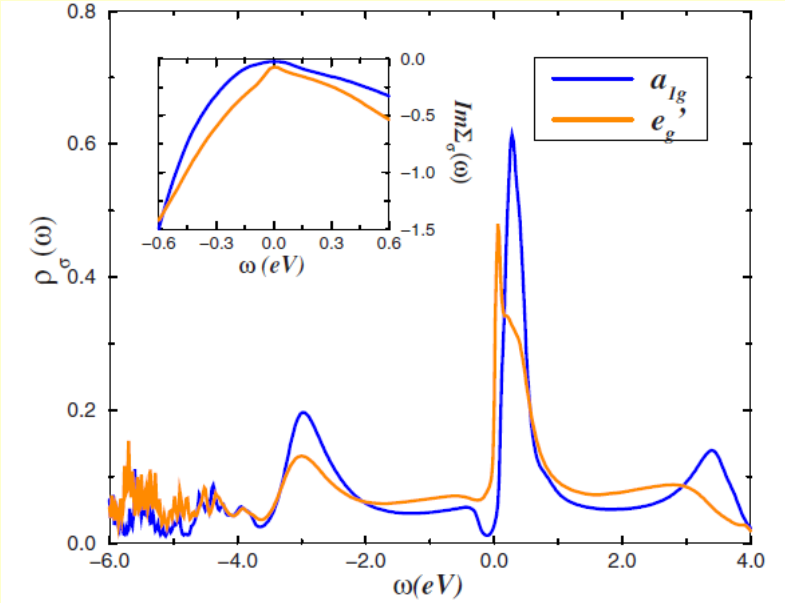

FIG. 2. (Color online) t_{2g}-resolved LDA+DMFT densities of states for $Hg_2Ru_2O_7$ in the high-T nFL phase, for U=5.5 eV and J_H=1 eV. Notice the orbital-selective (OS) nature of the metal, as well as the nFL character in the orbital-resolved self-energies (see inset).

L. Craco et al,
PRB 79, 075125 (2009)

Conclusions

- O1s core level PES show negligible changes across the MIT
- Tl 4f and Hg4f core levels show weak shape changes.
- Ru 3d PES show clear changes across the MIT in $Hg_2Ru_2O_7$ and $Tl_2Ru_2O_7$, with well-screened and poorly screened features.
- Valence band spectra and XAS of $Hg_2Ru_2O_7$ and $Tl_2Ru_2O_7$ show gap formation.
- MITs are of the Mott-Hubbard type in $Hg_2Ru_2O_7$ and $Tl_2Ru_2O_7$.
- MIT in $Hg_2Ru_2O_7$ does not show orbital ordering while $Tl_2Ru_2O_7$ show changes in XAS consistent with orbital ordering.